Trade-off assessment between controllability and energy savings in internally and externally heat integrated distillation structures

A. Miyazaki, J. Rafael Alcántara-Avila, K.-I. Sotowa, and T. Horikawa

Abstract— **Distillation is known as a separation process, which inherently entails high energy consumption. To alleviate this situation, heat integration between vapor streams at high pressure and liquid streams at low pressure have been proposed and extensively researched in the past decades. Most of these studies have been done at steady state, and little has been researched at dynamic state, particularly, when heat integration is done at locations other than condensers and reboilers in the columns. Thus, it is our aim to assess the trade-off between economic and/or energy savings and controllability at an early design stage by combining a design procedure, which minimizes the total annual cost, and an analysis at zero frequency, which calculates the theoretical control properties of distillation columns. The relative gain array (RGA) was used to determine the most appropriate pairing between controlled and manipulated variables while the singular value decomposition (SVD) technique was used to assess the theoretical control properties of conventional and heat-integrated structures. A ternary mixture with two different feed compositions was evaluated, the results showed that for an almost equimolar feed composition, the controllability can be improved by sacrificing the cost and energy savings if the number of intermediate heat exchangers is decreased while for a feed composition high in the intermediate component, the distillation column with the highest energy savings also attained the best controllability performance.**

I. INTRODUCTION

Distillation is widely used to separate liquid mixtures in the Chemical and Petrochemical industry. The Japanese agency for Natural Resources and Energy reported that the Chemical industry consumed 2,267 PJ in 2012 [1]. From this energy, around 40% is consumed by distillation columns [2]. To reduce the energy consumption in distillation columns, heat integration between vapor streams at high pressure and liquid streams at low pressure has been widely used [3]. Two types of heat integrations are studied in this work. External heat integration is defined as the heat integration between the vapor streams leaving a condenser at high pressure and the liquid stream leaving a reboiler at low pressure (Fig. 1 left) whereas internal heat integration is defined as the heat integration(s) at any stage(s) in a rectifying section at high pressure and any stage(s) in a stripping section at high pressure (Fig. 1 right).

Evaluations at steady state have shown that the combination of external and internal heat integration can attain economic and/or energy savings higher than only external heat integration for the separation of binary [4] and ternary [5] mixtures. Heat-integrated stages can be applied to Air Separation Units (ASU) to improve its thermodynamic efficiency and reduce the entropy production up to 31% [6]. Consequently as the number of heat-integrated stages increased, the entropy production in the rectifying section of the low pressure column reduced.

The authors are with the Department of Chemical Science and Technology, The University of Tokushima, 2-1 Minami Josanjima-cho, Tokushima 770-8506, Japan.
(Corresponding author to provide phone: +81-88-656-7425; fax: +81-88-656-7425; e-mail: alcantara@chem.tokushima-u.ac.jp).

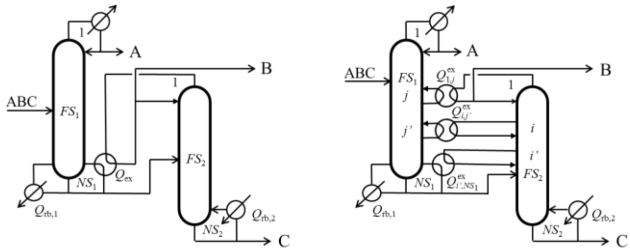

Figure 1. External and internal heat integrations

The design and control of external heat integration has been researched previously and it is rather straightforward since the heat integration is restricted at one location, the energy supplied by the condenser is equal to the energy reduced at the reboiler, and there are few candidate variables to be manipulated [7]. However, the design of distillation columns with internal heat integration depends on the number and locations of heat exchangers, and the amount of energy exchanged at every location. In addition, there are more candidate variables to be manipulated as well as controlled. As a result, a larger combinatorial problem must be solved. Therefore, its design at steady state, and the selection of the best control configuration at dynamic state are not trivial.

Previous researches have assessed the control properties of the distillation structure with the minimum cost and/or energy consumption at the steady state [4, 7], however, the relation between economic and/or energy savings and the control properties has not been explicitly assessed. Therefore, this research aims to quantify the trade-off between several distillation structures with minimal cost and/or energy consumption and their control properties at an early design stage.

II. DESIGN AT STEADY STATE

Distillation inherently consist of a system of nonlinear and nonconvex equations, in addition there are discrete variables such as the number of stages and feed location, therefore optimization approaches must solve a mixed-integer linear programming (MINLP) problems. In this work, nonlinearities and nonconvexities were solved in Aspen Plus 8.0 in combination with sensitivity analyses, which were used to optimize the integer variables for the base cases without heat integration, and the cases with only external heat integration. For the cases which considered internal heat integrations, because large combinatorial problems between stages arise, a Mixed Integer Linear Programming (MILP) was developed which embedded the results obtained in Aspen Plus 8.0 to find the best internal heat integration network.

The next subsections mention in detail the design procedure when the feed condition, product specifications, and operating pressure in each column are set in advance.

A. Conventional columns

1. Initialize the feed stage and number of stages, FS_k and NS_k, in each column k.
2. Minimize the value of the total annual cost (TAC) of a distillation sequence according to (1)

$$\begin{aligned} &\min\ TAC = EC / PT + OC * AO \\ &s.t. \\ &g(NS_1, NS_2, FS_1, FS_2, Q_{\mathrm{rb},1}, Q_{\mathrm{rb},2}) \geq 0, \end{aligned} \quad (1)$$

where EC and OC are the equipment cost and operation cost, PT is the payback time, AO is the number of annual operation hours. Q_{rb} is the reboiler duty.

B. External heat integration

1. Initialize FS_k and NS_k in each column k.
2. Minimize (2)

$$\begin{aligned} &\min\ TAC = EC / PT + OC * AO \\ &s.t. \\ &g(NS_1, NS_2, FS_1, FS_2, Q_{\mathrm{rb},1}, Q_{\mathrm{rb},2}, Q_{\mathrm{ex}}) \geq 0, \end{aligned} \quad (2)$$

where Q_{ex} is the energy exchanged between the high pressure vapor at the condenser and the low pressure liquid at the reboiler.

The aforementioned procedures can be readily done by solving the nonlinear problems in the process simulator and combining them with sensitivity analyses for each NS_k and FS_k, and a spreadsheet in Excel to calculate TAC.

C. Internal heat integration

1. Initialize FS_k and NS_k in each column k.
2. Minimize (3)

$$\begin{aligned} &\min\ TAC = EC / PT + OC * AO \\ &s.t. \\ &g(NS_1, NS_2, FS_1, FS_2, Q_{\mathrm{rb},1}, Q_{\mathrm{rb},2}, Y_{i,j}^{\mathrm{ex}}, Q_{i,j}^{\mathrm{ex}}) \geq 0, \end{aligned} \quad (3)$$

where $Y_{i,j}^{ex}$ is a binary variable which only becomes one when heat integration is realized between stages i in the high pressure column and j in the low pressure column, and $Q_{i,j}^{ex}$ is its exchanged energy.

This procedure solves the nonlinearities in the process simulator and the combinatorial problem for $Y_{i,j}^{ex}$ by adopting the MILP mathematical formulation in one of our previous researches [4] after minor modifications. From the shown design procedures, it can be seen that the design of internal heat integration is much more complex than the rest.

Equation (4) breaks down the terms for EC and OC as follows:

$$\begin{aligned} EC &= (C^{tower} + C^{tray} + C^{con} + C^{reb} + C^{ex})(1 + C^{MI}) \\ OC &= C^{cool}(Q_{\mathrm{cn},1} + Q_{\mathrm{cn},2}) + C^{heat}(Q_{\mathrm{rb},1} + Q_{\mathrm{rb},2}) \end{aligned} \quad (4)$$

where C^{tower}, C^{tray}, C^{con}, C^{reb}, C^{ex} are the purchase cost of the tower, trays, condensers, reboilers and additional heat exchangers. C^{MI} is the maintenance and instrumentation cost. C^{cool} and C^{heat} are the cooling and heating utility cost per unit amount of energy transferred. Finally, Q_{cn} is the condenser duty.

Calculations for the equipment cost and operation cost were based on the Guthrie method and reported data adopted from [8]. Table I summarizes the used parameters and conditions for cost calculations.

III. Control Properties

Distillation columns exhibit interaction between output and input variables, which means that a change in any input affects more than one output. In addition, some output-input combinations are more sensitive than others, and they might lead to high disturbances and difficulty to control the process. The following subsections describe the control properties studied in this work.

A. Relative Gain Array

The relative gain array (RGA) is used to determine the best output-input variable pairing that minimizes the interaction in a multivariable system. For a system with three controlled and three manipulated variables, the RGA can be expressed as

$$\Lambda = \begin{bmatrix} \lambda_{11} & \lambda_{12} & \lambda_{13} \\ \lambda_{21} & \lambda_{22} & \lambda_{23} \\ \lambda_{31} & \lambda_{32} & \lambda_{33} \end{bmatrix}. \quad (5)$$

Each element λ_{ij} represents the ratio of the open loop gain of i and j to the open loop gain of i when all the other loops are closed. Each element can be calculated by (6)

$$\begin{aligned} \lambda_{ij} &= K_{ij} r_{ij} \\ r_{ij} &= (K_{ij}^{-1})^{\mathrm{T}} \end{aligned} \quad (6)$$

where K_{ij} is the output-input open loop gain.

TABLE I. ASSUMPTIONS USED IN THE *EC* AMD *OC* CALCULATIONS

Parameter	**Value**
Material construction for towers	Carbon steel
Material construction for trays (type)	Carbon steel (Sieve)
Material construction for condensers and side exhangers	Carbon steel/ Carbon steel
Material construction for reboilers	Carbon steel/ Stainless steel
Maintenance and instrumentation cost (C^{MI})	18% of the purchase cost
Cooling water cost, [$/MW]	0.86
Steam cost, [$/MW]	11.83
Heat transfer coefficient for condensers and side exchangers [kW/m^{2}K]	0.7
Heat transfer coefficient for reboilers [kW/m^{2}K]	1.0

A value of λ_{ij} close to one is desirable because this implies that there is not interaction between output *i* and input *j* while zero or negative values must be avoided since those values lead to unstable pairings, thus control is not possible. Large values of λ_{ij} imply that the system is difficult to control due to strong interaction and sensitivity to uncertainty [9].

B. Singular Value Decomposition

The singular value decomposition (SVD) is a factorization of a real or complex matrix into three matrices as shown in (7)

$$M = W \Sigma V^{\mathrm{T}} \tag{7}$$

where *M* is a given matrix, *W* and *V* are orthogonal matrices, and Σ is a diagonal matrix of singular values.

From the control point of view, the maximum and minimum singular values of Σ, $\sigma_{\max}$ and $\sigma_{\min}$ respectively, are important since they denote the maximum and minimum gains of the systems output as the input is varied [10].

The condition number (*CN*) is defined as the ratio of the maximum and minimum singular value

$$CN = \sigma_{\max} / \sigma_{\min} \,, \tag{8}$$

and it represents the sensitivity of the system to input uncertainty.

Large values of *CN* must be avoided because they imply that the system is ill-conditioned. If the system is almost singular, the computation of its inverse, and its solution is susceptible to large numerical errors. A matrix that is not invertible has $\sigma_{\min}$ equal to zero, therefore of $\sigma_{\min}$ represents the system invertibility, and values close to zero must also be avoided.

IV. CONTROLLABILITY AT ZERO FREQUENCY

The design of distillation columns with internal heat integration is more complex than typical external heat integration and conventional columns not only from the design point of view, but also from the dynamic point of view because there are more locations subject to heat integration, thus more process interactions due to an increase in the number of manipulated and controlled variables. Studies at steady state can quantify the cost, energy consumption or entropy production, however studies at dynamic state can deepen the knowledge about how processes behave under fluctuations. Therefore, the best pairing of output-input variables and their sensitivity to uncertainties can be known at an early design stage through steady-state analyses at zero frequency, and subsequently perform a complete analysis in the frequency domain.

Table II shows the candidate controlled variables *y* (hereinafter called output) and manipulated variables *u* (hereinafter called input) for the distillation sequence with only external heat integration, which is shown in Fig. 2.

For internal heat integration, additional outputs and inputs are considered and shown in Table III for a direct distillation sequence with internal heat integration at three locations. In addition, Fig. 3 shows a schematic representation of the outputs and inputs in Tables II and III.

TABLE II. CANDIDATE VARIABLES FOR EXTERNAL HEAT INTEGRATION

Variable	**Description, units**	**Identifier**
y_1	Mol purity of A, (-)	X_A
y_2	Mol purity of B, (-)	X_B
y_3	Mol purity of C, (-)	X_C
u_1	Reflux ratio of column 1, (-)	RR_1
u_2	Reboiler duty of column 1, (kW)	QR_1
u_3	Reflux ratio of column 2, (-)	RR_2
u_4	Reboiler duty of column 2, (kW)	QR_2

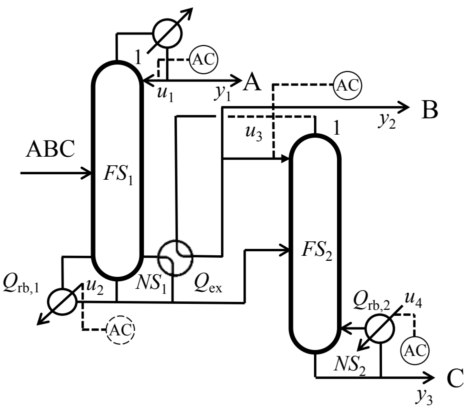

Figure 2. Output and input variables for external heat integration

TABLE III. ADDITIONAL CANDIDATE VARIABLES FOR INTERNAL HEAT INTEGRATION

Variable	**Description, units**	**Identifier**
y_4	Temperature on Tray *i*	T_i
y_5	Temperature on Tray *i'*	$T_{i'}$
y_6	Temperature on Tray *j*	T_j
y_7	Temperature on Tray *j'*	$T_{j'}$
u_5	Heat exchanged between stages 1 and *j*	HX_1
u_6	Heat exchanged between stages *i* and *j'*	HX_2
u_7	Heat exchanged between stages *i'* and NS_1	HX_3

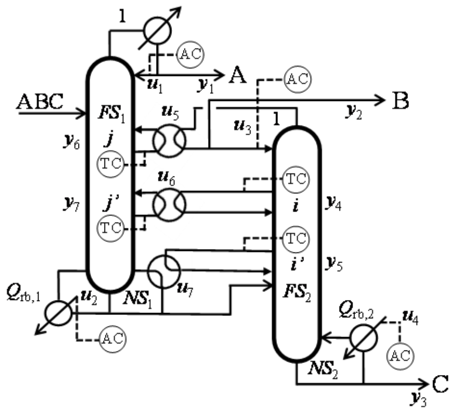

Figure 3. Input and output variables for internal heat integration

V. DESIGN AND CONTROL ASSESSMENT PROCEDURE

This section explains the adopted procedure to find the best open loop pairing at steady state for optimal distillation sequences as follows:

1. Solve the optimization problem described in II*.
2. Select the necessary outputs y_i to control.
3. Select u_j inputs equal to the number of selected y_i.
4. Calculate the open loop steady-state gain matrix K_{ij}.
5. Compute the RGA, *CN*, and $\sigma_{\min}$.
6. Repeat step 4 through 6 for different sets of u_j until all combinations are exhausted, and record all the results.
7. Select the best output-input pairing with the minimum *CN*.
8. Repeat step 1 through 7 for each optimal distillation structure, and assess the trade-off between economic and energy savings, and controllability based on the values of *CN*, and $\sigma_{\min}$.

*For conventional and externally heat-integrated distillation columns there is a unique solution, however, for internally heat-integrated distillation columns several optimal solutions are taken.

VI. CASE STUDY

The separation of a ternary mixture was taken as case study. The assumptions in Table I were adopted. Table IV shows the two feed conditions and product specifications for the separation of the ternary mixture. The assumed *PT* was 10 years, and *AO* was 8000 hours.

TABLE IV. FEED CONDITION AND PRODUCT SPECIFICATIONS

Component (ID)	F1 (kmol/h)	F2 (kmol/h)	Product mol fraction (-)
Cyclopentane (A)	40	25	0.98
Benzene (B)	30	50	0.98
Toluene (C)	30	25	0.98

VII. RESULTS AND DISCUSSION

All the possible distillation sequences for the separation of the ternary mixture were evaluated, and the direct sequence exhibited the lowest *TAC* for both feed compositions.

Table V shows the RGA and SVD results for all the possible output-input combinations to control a distillation column without heat integration. The best pairing for F1 is to manipulate RR_1, RR_2 and QR_2 while for F2 is to manipulate QR_1, QR_2 and RR_2 to control X_A, X_B, and X_C, respectively.

TABLE V. PAIRING AND CONTROL PROPIERTIES FOR THE CONVENTIONAL DISTILLATION SEQUENCE

Feed	Output-input pairing	RGA (λ_{ij})	SVD	
			CN	$\sigma_{\min}$
F1	y_1-u_1;y_2-u_3;y_3-u_4	1.00;0.91;0.91	24.56	0.01
	y_1-u_2;y_2-u_3;y_3-u_4	1.00;0.91;0.91	33.06	0.09
F2	y_1-u_2;y_2-u_4;y_3-u_3	1.00;0.95;0.95	2.06	0.69
	y_1-u_2;y_2-u_4;y_3-u_1	1.00;1.05;1.05	2.79	0.56

When external and internal heat integrations are enforced, the direct sequence also realized the minimum *TAC* for both feed compositions. Table VI shows the RGA and SVD results for all the best and second best output-input combinations of each feed composition to control a distillation column with only external heat integration. The best pairing for F1 is to manipulate RR_1, RR_2 and QR_2 while for F2 is to manipulate QR_1, RR_2 and RR_1 to control X_A, X_B, and X_C, respectively.

TABLE VI. PAIRING AND CONTROL PROPIERTIES FOR THE DISTILLATION SEQUENCE WITH EXTERNAL HEAT INTEGRATION

Feed	Output-input pairing	RGA(λ_{ij})	SVD	
			CN	$\sigma_{\min}$
F1	y_1-u_1;y_2-u_3;y_3-u_4	1.00;1.25;1.25	13.32	0.18
	y_1-u_2;y_2-u_3;y_3-u_4	1.00;1.25;1.25	15.10	0.20
F2	y_1-u_2;y_2-u_3;y_3-u_1	1.00;1.16;1.16	7.49	0.26
	y_1-u_2;y_2-u_4;y_3-u_1	1.00;0.64;0.64	8.97	0.32

For F1, the value of *CN* is lower and that of $\sigma_{\min}$ is higher than those when heat integration is not realized. These results imply that the externally heat-integrated sequence in F1 has better controllability, however, for F2, the values of *CN* and $\sigma_{\min}$ are higher when heat integration is realized. These results imply that the externally heat-integrated sequence in F2 has worse controllability.

In case of internal heat integration, the optimal and two suboptimal solutions were taken to assess its controllability for each feed composition. Fig. 4 shows the optimal distillation sequence with internal heat integration for F1 while Fig. 5 shows it for F2. These sequences realized heat integration at two locations. y_4 and y_5 represent the temperature at stage 1 and 6 for F1, and stages 1 and 3 for F2 in the high pressure column, respectively. y_6 and y_7 represent the temperature at stages 32 and 33 for F1, and stages 32 and 34 for F2 in the low pressure column, respectively. u_5 and u_6

are the amount of energy exchanged through internal heat integration. Table VII shows the RGA and SVD results for the possible output-input combinations to control the sequence. From these results, the best pairing for F1 is to manipulate $Q^{ex}_{6,33}$, RR_1 and QR_2 while for F2 is to manipulate RR_1, QR_2 and $Q^{ex}_{3,34}$ to control X_A, X_B, and X_C, respectively. In addition, for F1 RR_2 and $Q^{ex}_{1,32}$ are used to control the temperature at stages 6 and 33 while for F2 $Q^{ex}_{1,32}$ and QR_1 are used to control the temperature at stages 1 and 32, respectively.

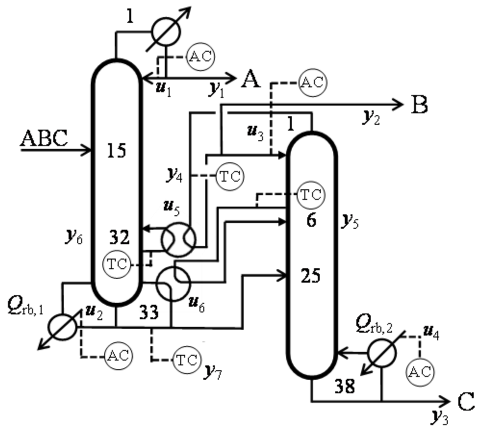

Figure 4. Optimal sequence with two heat-integrated stages for F1

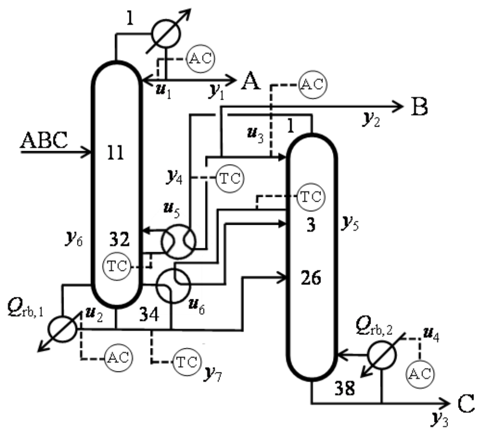

Figure 5. Optimal sequence with two heat-integrated stages for F2

TABLE VII. PAIRING AND CONTROL PROPIERTIES FOR THE OPTIMAL DISTILLATION SEQUENCE WITH TWO HEAT-INTEGRATED STAGES

Feed	Output-input pairing	RGA (λ_{ij})	SVD	
			CN	σ_{min}
F1	y_1-u_6;y_2-u_3;y_3-u_4;y_7-u_5;y_5-u_1	1.02;0.70;3.28;1.17;3.26	1062	0.17
	y_1-u_6;y_2-u_1;y_3-u_4;y_7-u_5;y_4-u_3	1.01;1.89;3.34;1.17;0.64	3181	0.06
F2	y_1-u_1;y_2-u_4;y_3-u_6;y_6-u_2;y_4-u_5	0.83;4.58;2.17;18.71; 18.77	2510	0.01

Table VIII shows the RGA and SVD results for the possible output-input combinations in F1 and F2 to control a suboptimal distillation sequence with two heat-integrated stages. For F1, stage 28 in the low pressure column and stage 4 in the high pressure column are heat-integrated while for F2, stage 26 in the low pressure column and stage 11 in the high pressure column are heat-integrated.

From the results in Table VIII, the best pairing for F1 is to manipulate $Q^{ex}_{4,33}$, RR_2 and QR_2 while for F2 is to manipulate RR_1, QR_1 and $Q^{ex}_{10,34}$ to control X_A, X_B, and X_C, respectively. In addition, for F1, $Q^{ex}_{1,28}$ and RR_1 are used to control the temperature at stages 1 and 33 while for F2, QR_2 and $Q^{ex}_{1,26}$ are used to control the temperature at stages 1 and 26, respectively.

A comparison between the optimal and suboptimal solutions shows how the controllability worsens when heat integration occurs at locations far from the condenser in the high pressure column and from the reboiler in the low pressure column.

Table IX shows the RGA and SVD results for the possible output-input combinations in F1 and F2 to control a suboptimal distillation sequence with one heat-integrated stage. For F1 and F2, stage 27 in the low pressure column is heat-integrated.

From the results in Table IX, the best pairing for F1 is to manipulate RR_1, RR_2 and QR_2 while for F2 is to manipulate $Q^{ex}_{1,27}$, RR_1, and QR_2 to control X_A, X_B, and X_C, respectively. In addition, for F1, $Q^{ex}_{1,27}$ is used to control the temperature at stage 27 while for F2 QR_1 is used to control the temperature at stage 27, respectively.

Tables X and XI summarize *EC*, *OC*, *TAC*, energy consumption, and economic and energy savings, for the conventional and heat-integrated distillation structures.

TABLE VIII. PAIRING AND CONTROL PROPIERTIES OF A SUBOPTIMAL DISTILLATION SEQUENCE WITH TWO HEAT-INTEGRATED STAGES

Feed	Output-input pairing	RGA (λ_{ij})	SVD	
			CN	σ_{min}
F1	y_1-u_6;y_2-u_3;y_3-u_4;y_7-u_1;y_4-u_5	1.00;7.92;6.04;5.85;6.11	2991	0.02
	y_1-u_1;y_2-u_3;y_3-u_4;y_7-u_5;y_5-u_6	1.78;7.12;5.85;2.87;0.78	7066	0.02
F2	y_1-u_1;y_2-u_2;y_3-u_6;y_6-u_5;y_4-u_4	7.17;1.14;1.59;7.53;2.00	91929	3E-4

TABLE IX. PAIRING AND CONTROL PROPIERTIES FOR A SUBOPTIMAL DISTILLATION SEQUENCE WITH ONE HEAT-INTEGRATED STAGE

Feed	Output-input pairing	RGA(λ_{ij})	SVD	
			CN	σ_{min}
F1	y_1-u_1;y_2-u_3;y_3-u_4;y_6-u_5	3.69;1.24;1.24;3.69	180	0.19
F2	y_1-u_5;y_2-u_1;y_3-u_4;y_6-u_2	127;0.42;1.93; 43.0	7570	1.6E-3

TABLE X. DETAILED EQUIPMENT AND UTILITY COST COMPARISON

Feed		C^{tower}+ C^{tray} (k$)	C^{con} (k$)	C^{reb} (k$)	C^{ex} (k$)	C^{cool} (k$)	C^{heat} (k$)
F1	Base case	259.0	322.3	108.4	---	10.4	153.5
	E-HX	300.0	392.3	106.0	44.8	5.0	87.9
	Fig. 4	300.3	99.8	106.0	46.1	7.5	80.4
	2-HI	299.7	100	105.6	46.1	7.0	81.0
	1-HI	290.9	130.9	101.2	46.8	9.6	93.8
F2	Base case	297.1	141.2	141.2	---	11.2	156.3
	E-HX	304.6	96.2	96.2	46.3	6.5	100.2
	Fig. 5	319.7	96.5	96.5	47.2	6.4	98.7
	2-HI	323.0	100.0	100.0	48.8	6.6	100.9
	1-HI	322.4	136.3	136.3	43.7	11.7	109.8

TABLE XI. COMPARISON BETWEEN *TAC* AND ENERGY CONSUMPTION

Feed		*TAC* (k$/y)	*TAC* savings (%)	$Q_{rb,1}$+$Q_{rb,2}$ (kW)	Energy savings (%)
F1	Base case	241.6	---	1622.5	---
	E-HX	180.3	25.4	929.2	42.7
	Fig. 4	175.8	27.2	850.3	47.6
	2-HI	175.8	27.2	856.1	47.2
	1-HI	192.1	20.5	881.3	45.7
F2	Base case	251.6	---	1652.1	---
	E-HX	196.5	21.9	1059.2	35.9
	Fig. 5	198.0	21.3	1043.7	36.8
	2-HI	201.7	19.8	1066.8	35.4
	1-HI	219.2	12.9	1160.3	29.8

In the tables above, the base case is the conventional sequence without heat integration, E-HX is the one with external heat integration, 2-HI is the suboptimal sequence with two heat-integrated stages and 1-HI is the suboptimal sequence with one heat-integrated stage.

Although external heat integration had better values of *CN* and $\sigma_{\min}$ than those with heat-integrated stages, in most cases, the latter had better cost and/or energy savings than the former. For the studied feed compositions, the optimal solution with heat-integrated stages also showed the best controllability. It was observed that for heat-integrated stages near the condenser and reboiler, the controllability and the energy savings were improved. For distillation sequences with one heat-integrated stage, the controllability was remarkable improved, although the economic and energy savings were deteriorated.

VIII. CONCLUSION

A design and control assessment procedure based on process simulation and optimization combined with numerical analyses at zero frequency was presented to evaluate the trade-off between economic, energy and controllability in internally and externally heat integrated distillation structures. Two feed compositions were studied to prove the robustness of the proposed procedure, and, in both cases, all the solutions with heat integrations attained economic and energy savings when compared with the base case. From the evaluated control properties at steady state, all the presented solutions can be controlled, however, the control properties deteriorated as the economic and energy savings improved.

In addition, as the number of internal heat integrations increased, the control properties deteriorated due to higher interaction between variables. Therefore, internally heat-integrated distillation sequence with few heat integrations would be preferred from the control point of view.

For internally heat-integrated distillation structures, in both feed conditions, the controllability was drastically worsen when heat integration occurred at stages away from the condenser in the high pressure column and/or the reboiler in the low pressure column.

From the economic analysis, the *EC* for internally heat-integrated distillation sequences was higher than that for externally heat-integrated distillation sequences due to the increase of one or two heat exchangers, however, the *OC* for the former was lower than that for the latter.

Our findings suggest that there is a trade-off between economic, energy and controllability in distillation sequences with internal heat integration. Although a reduced number of internal heat integrations might not lead to the lowest cost or energy consumption, it can still offer an attractive solution with economic and energy savings which can be control without great effort.

REFERENCES

[1] http://www.enecho.meti.go.jp/topics/hakusho/2012/2-1.pdf

[2] K. Hirata, "Heat integration of distillation column," *Chem. Eng. Trans.*, vol. 18, pp. 39–44, 2009.

[3] M. J. Andrecovich, and A. W. Westerberg, "An MILP formulation for heat-integrated distillation sequence synthesis," *AIChE J.*, vol. 31, no. 9, pp.1461–1474, Sep. 1985.

[4] X. Zhang, K. Huang, H. Chen, and S. Wang, "Comparing three configurations of the externally heat-integrated double distillation columns (EHIDDiCs)," *Comput. Chem. Eng*., vol. 35, no. 10, pp. 2017–2033, Oct. 2011.

[5] J. R. Alcántara-Avila, M. Kano, and S. Hasebe, "New synthesis procedure to find the optimal distillation sequence with internal and external heat integrations," *Ind. Eng. Chem. Res*., vol. 52, no. 13, pp. 4851–4862, Apr. 2013.

[6] Van der Ham, L. V., and S. Kjelstrup, "Improving the Heat Integration of Distillation Columns in a Cryogenic Air Separation Unit," *Ind. Eng. Chem. Res.,* vol. 50, no. 15, pp. 9324–9338, Jun. 2011.

[7] P. Mizsey, N. T. Hau, N. Benko, I. Kalmar, and Z. Fonyo, "Process control for energy integrated distillation schemes," *Comput. Chem. Eng*., vol. 22, Supplement, pp. S427–S433, 1998.

[8] W. D. Seider, J. D. Seader, D. R. Lewin, and S. Widagdo, *Product and process design principles*. Asia: John Wiley & Sons, 3rd Ed, 2010, pp. 557–604.

[9] http://www.nt.ntnu.no/users/skoge/vgprosessregulering/papers-pensum/ch3-ch10-2ndedition.pdf

[10] S. Skogestad, and M. Morari, "Understanding the dynamic behavior of distillation columns," *Ind. Eng. Chem. Res*., vol. 27, no. 10, pp. 1848–1862, Oct. 1988.